

## Supporting Information

### Thermal, Structural and Dynamic Properties of Ionic Liquids and Organic Ionic Plastic Crystals with a Small Ether-Functionalised Cation

*Anna Warrington,<sup>a,b</sup> Colin S. M. Kang,<sup>a,b</sup> Craig Forsyth,<sup>c</sup> Cara M. Doherty,<sup>d</sup> Durga Acharya,<sup>d</sup> Luke A. O'Dell,<sup>e</sup> Nanditha Sirigiri,<sup>a</sup> Joshua Boyle,<sup>b</sup> Oliver E. Hutt,<sup>b</sup> Maria Forsyth<sup>a</sup> and Jennifer M. Pringle<sup>a\*</sup>*

<sup>a</sup> Institute for Frontier Materials, Deakin University, Burwood, VIC 3125, Australia

<sup>b</sup> Boron Molecular, 500 Princes Hwy, Noble Park, VIC 3174, Australia

<sup>c</sup> School of Chemistry, Monash University, Wellington Road, Clayton, VIC 3800, Australia

<sup>d</sup> Commonwealth Scientific and Industrial Research Organisation (CSIRO), Manufacturing, Clayton, 3168, VIC, Australia

<sup>e</sup> Institute for Frontier Materials, Deakin University, Geelong, VIC 3216, Australia

\*Email: [jenny.pringle@deakin.edu.au](mailto:jenny.pringle@deakin.edu.au)

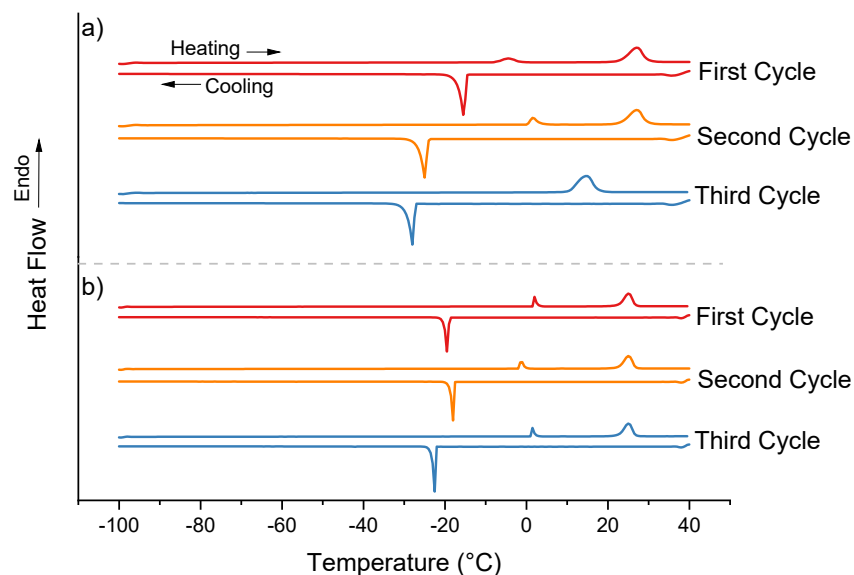


**Figure S1.** DSC trace of [N<sub>111,101</sub>][TFSI] at a) 10 °C min<sup>-1</sup> and b) 2 °C min<sup>-1</sup> for heating and cooling cycles.

The DSC analysis of the IL [N<sub>111,101</sub>][TFSI] was first measured using a cooling and heating rate of 10 °C/min (Figure S1a). In the first and second heating run, a peak was seen at between -3 °C and 0 °C, and a second peak was seen at 23 °C. In the third heating run, these two peaks merged into one larger peak with almost the same total entropy, seen at 11 °C. To assign, with reliability, these peaks to their corresponding transitions, a subsequent DSC measurement was conducted with slow cooling to -100 °C at 2 °C /min, before heating at 2 °C/min (Figure S1b). In the second run, the TFSI-based salt displayed one solid-solid transition at -3 °C with the formation of a metastable phase and a T<sub>m</sub> of the metastable phase at 23 °C.

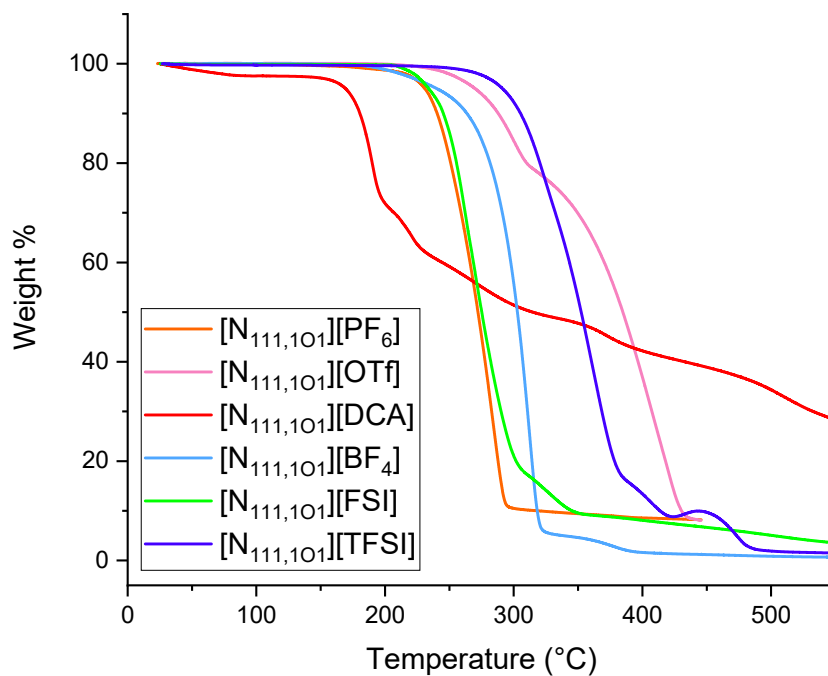


**Figure S2.** Thermogravimetric analysis of the [N<sub>111,101</sub>]<sup>+</sup> based salts.

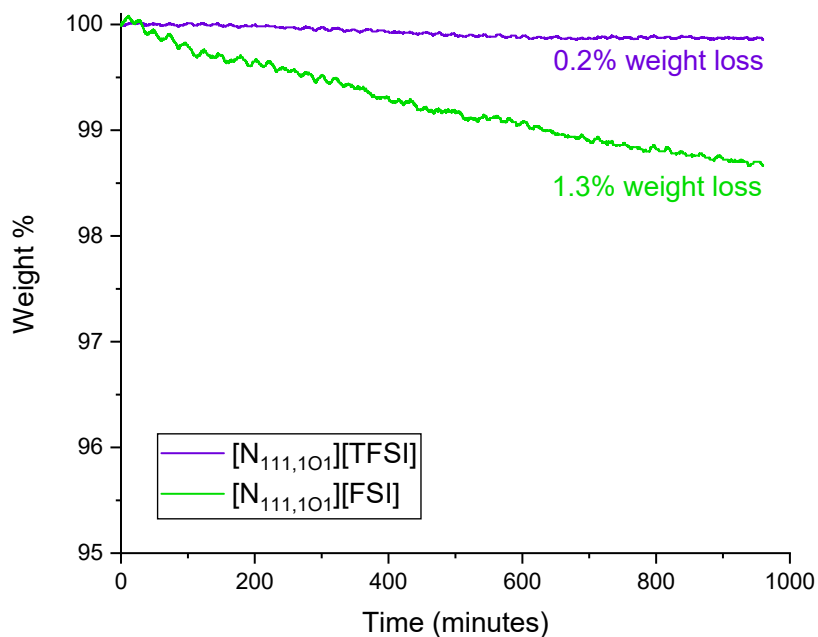


**Figure S3.** Isothermal thermogravimetric analysis of [N<sub>111,101</sub>][TFSI] and [N<sub>111,101</sub>][FSI]. The samples were held at 80 °C for 16 hours (960 minutes). [N<sub>111,101</sub>][TFSI] and [N<sub>111,101</sub>][FSI] displayed weight loss of 0.2 and 1.3 %, respectively.

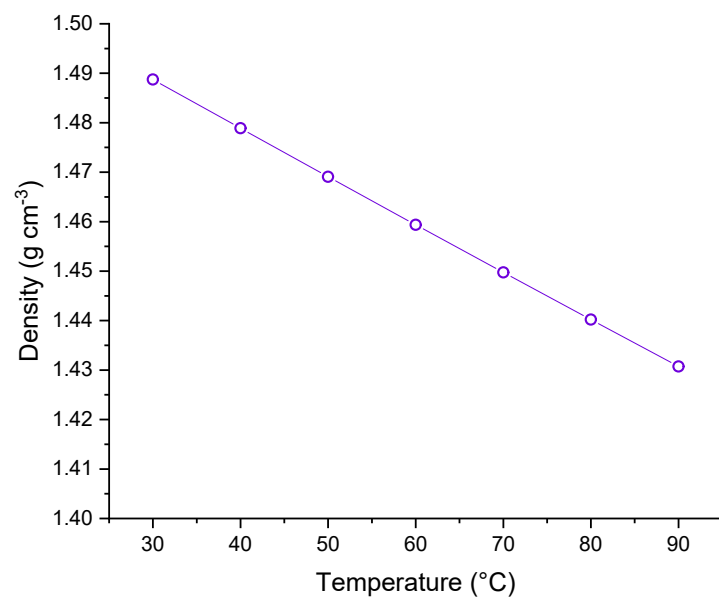


**Figure S4.** Temperature dependent density of [N<sub>111,101</sub>][TFSI].

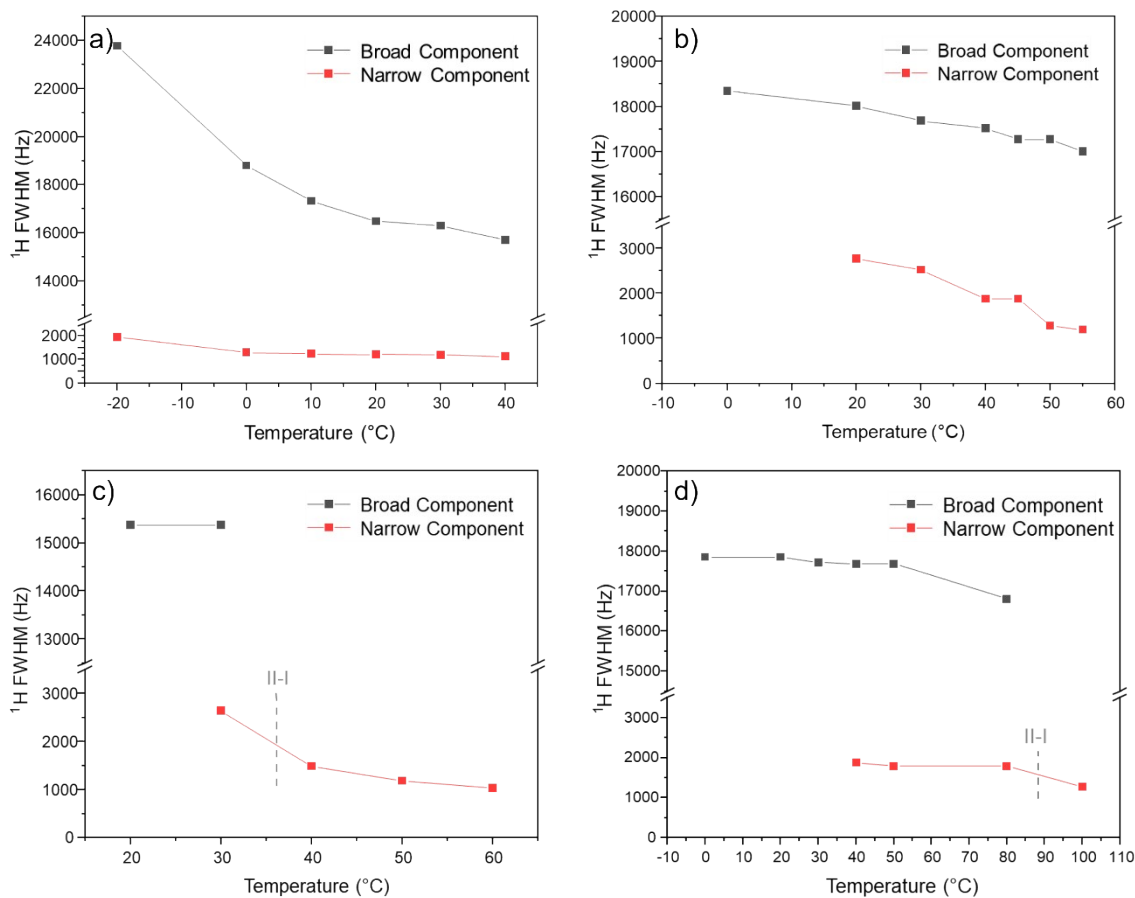


**Figure S5.** Solid-state NMR  $^1\text{H}$  Full Width at Half Maximum (FWHM) line widths against temperature for a)  $[\text{N}_{111,101}][\text{DCA}]$ , b)  $[\text{N}_{111,101}][\text{BF}_4]$ , c)  $[\text{N}_{111,101}][\text{OTf}]$  and d)  $[\text{N}_{111,101}][\text{PF}_6]$ .

*Note:*  $[\text{N}_{111,101}][\text{FSI}]$   $^1\text{H}$  FWHM line widths in phase I could not be determined as it displayed an asymmetric peak. As temperature was increased, three peaks became distinguishable which correspond to the three  $^1\text{H}$  environments present, as seen in solution-state NMR.

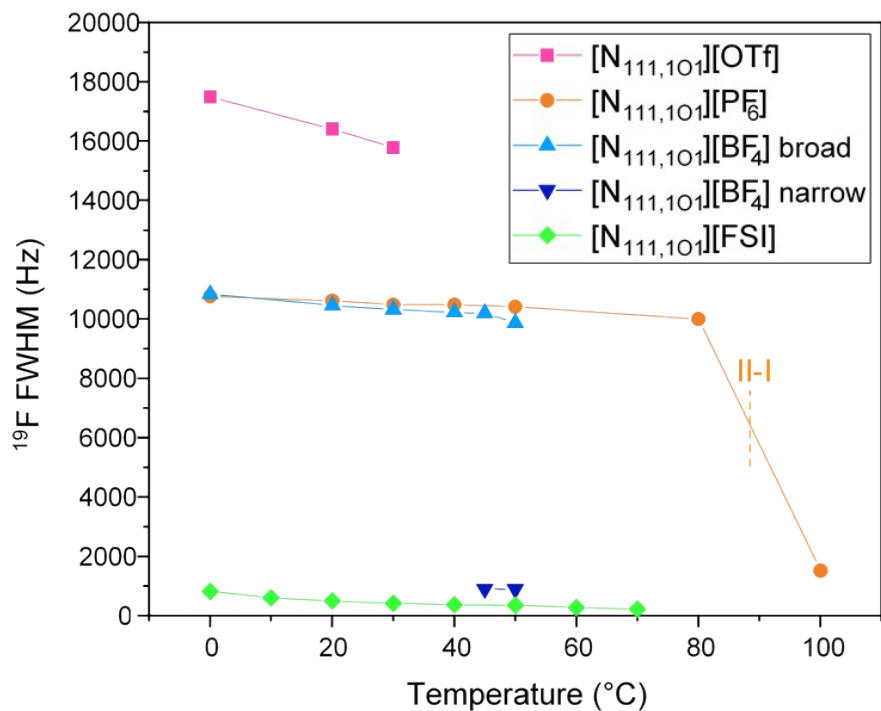


**Figure S6.** Solid-state NMR <sup>19</sup>F FWHM line width values against temperature for solid materials with fluorinated anions. [N<sub>111,101</sub>][OTf] values presented are in phase II only as the phase I <sup>19</sup>F spectrum presented complex CSA patterns. [N<sub>111,101</sub>][BF<sub>4</sub>] displayed a broad and narrow peak from 20 °C but this peak could only be accurately integrated from 45 °C.

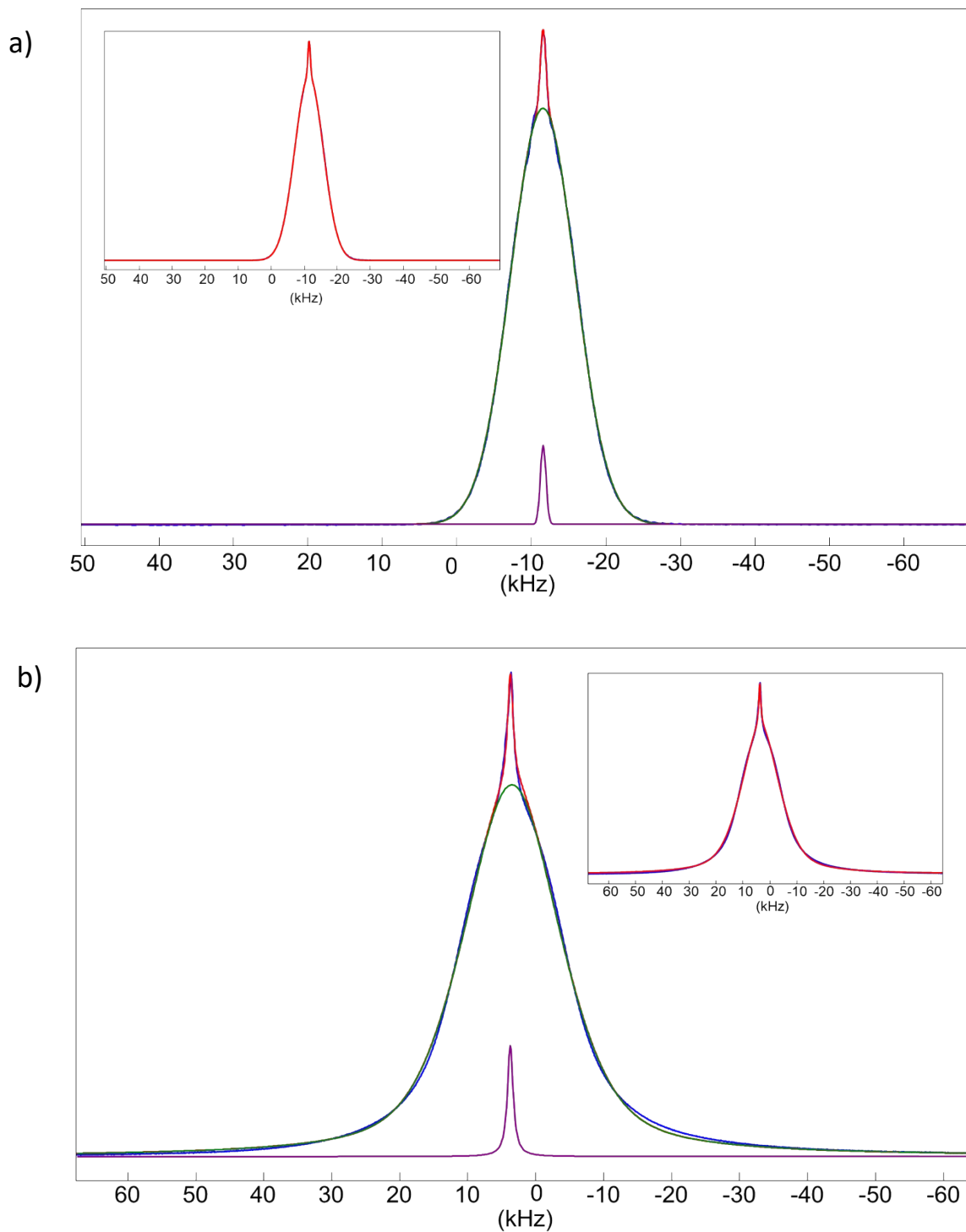


**Figure S7.** Solid-state NMR deconvolution fitting using DMfit software of a)  $^{19}\text{F}$   $[\text{N}_{111,101}][\text{BF}_4]$  at  $40\text{ }^\circ\text{C}$  and b)  $^1\text{H}$   $[\text{N}_{111,101}][\text{BF}_4]$  at  $40\text{ }^\circ\text{C}$ . The green peak represents the broad components and the

purple peaks represent the narrow component. The red peak is the cumulative peak and the NMR spectra are blue. The insets show the cumulative peak only, on top of the NMR spectrum.

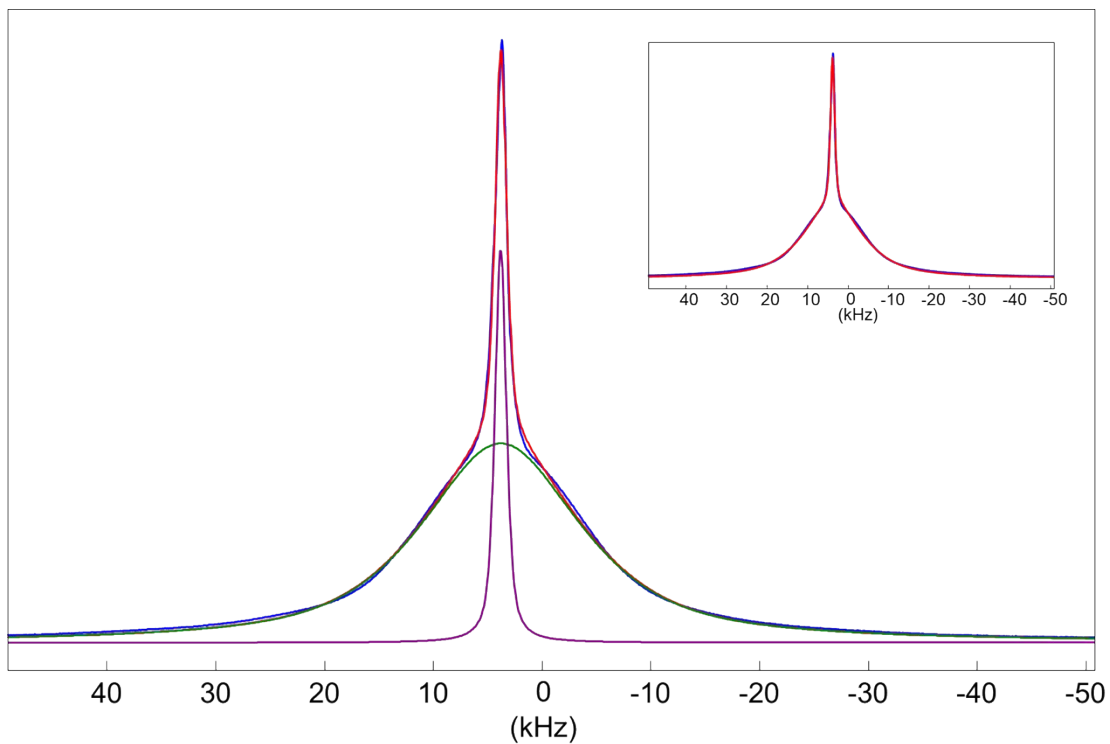


**Figure S8.** Solid-state NMR deconvolution fitting using DMfit software of  $^1\text{H}$  [ $\text{N}_{111,101}$ ][DCA] at 40 °C. The green peak represents the broad component and the purple peak represent the narrow component. The red peak is the cumulative peak and the NMR spectrum is blue. The inset show the cumulative peak only, on top of the NMR spectrum.

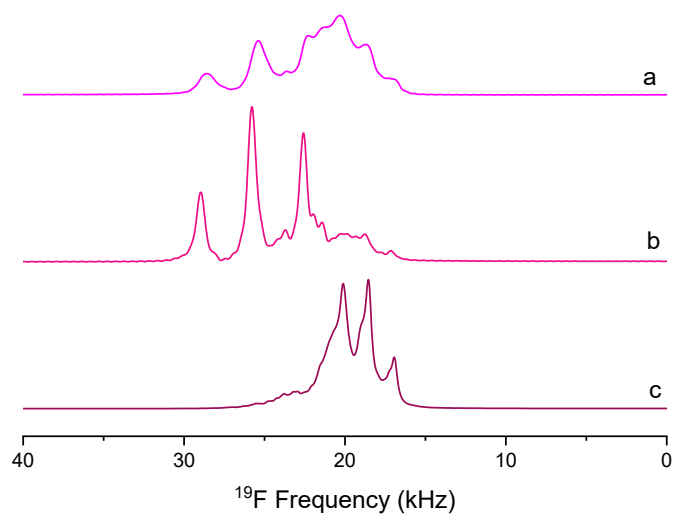


**Figure S9.**  $^{19}\text{F}$  static NMR spectra of  $[\text{N}_{111,101}][\text{OTf}]$  at  $60\text{ }^\circ\text{C}$ . The different spectra were recorded after a) the sample was heated to  $60\text{ }^\circ\text{C}$  from the ambient temperature, b) the sample was cooled to  $0\text{ }^\circ\text{C}$  then heated to  $60\text{ }^\circ\text{C}$ , and c) the sample was heated to melt at  $80\text{ }^\circ\text{C}$  and cooled to  $60\text{ }^\circ\text{C}$ .

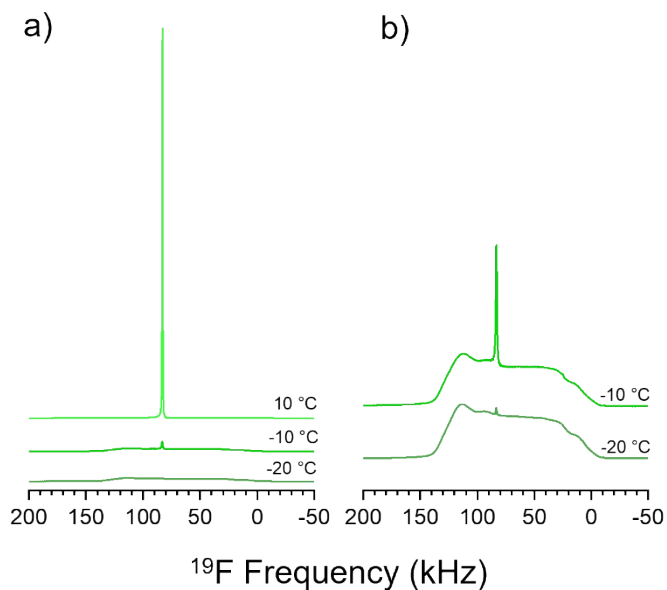


**Figure S10.**  $^{19}\text{F}$  static NMR spectra of  $[\text{N}_{111,101}][\text{FSI}]$  at a)  $-20\text{ }^\circ\text{C}$ ,  $-10\text{ }^\circ\text{C}$  and  $10\text{ }^\circ\text{C}$  on same y-axis scale, and b)  $-20\text{ }^\circ\text{C}$  and  $-10\text{ }^\circ\text{C}$  on the same scale.

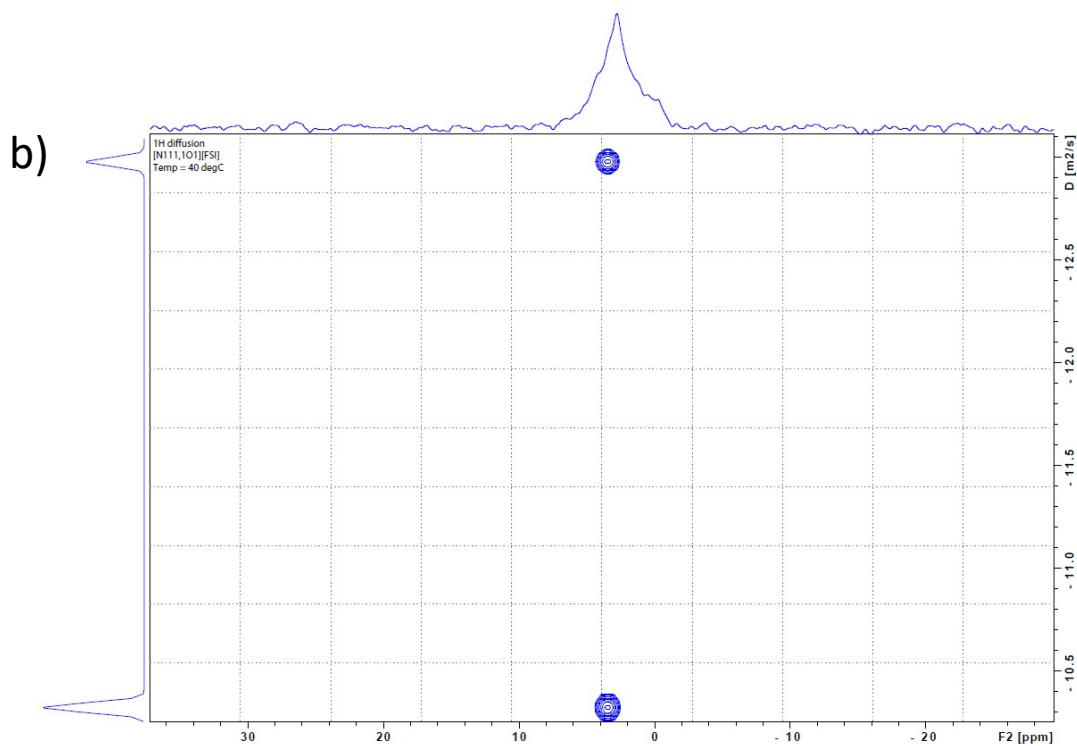
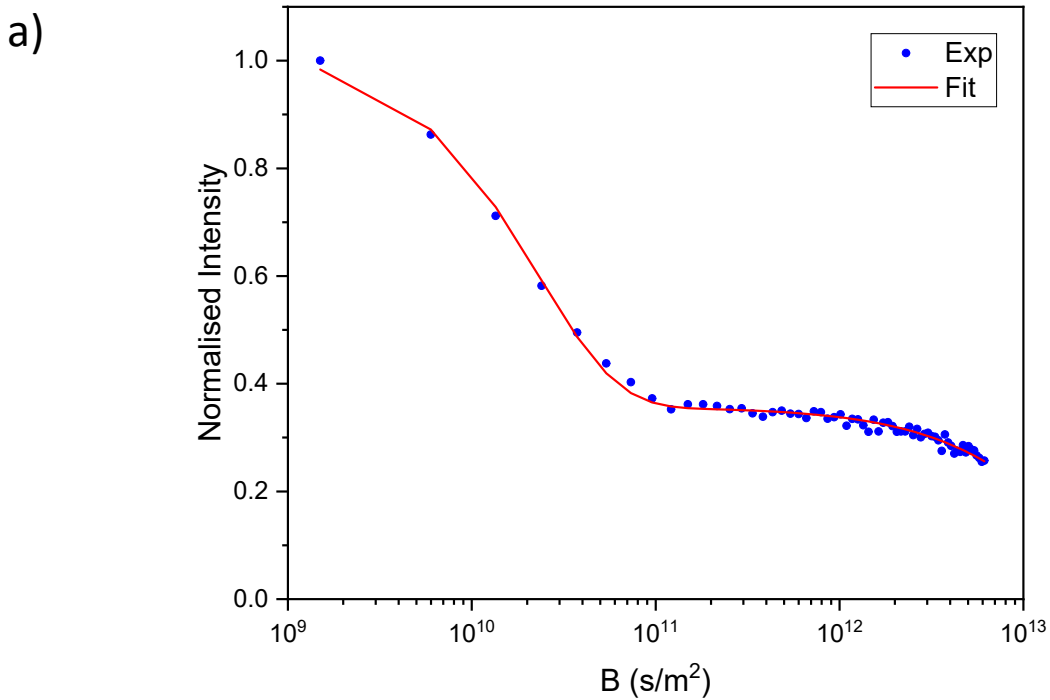


**Figure S11.** <sup>1</sup>H PFG data for [N<sub>111,101</sub>][FSI] displaying two diffusive species a) <sup>1</sup>H PFG NMR

attenuation at 40 °C, where  $B$  is a prefactor defined by  $B = \gamma^2 g^2 \delta^2 \left( \Delta - \frac{\delta}{3} \right)$  where  $\gamma$  is the nuclear

gyromagnetic ratio,  $g$  is the gradient strength,  $\Delta$  is the diffusion time and  $\delta$  is the gradient pulse

length.  $B$  is shorthand for the Stejskal Tanner equation  $S = S_0 e^{-\gamma^2 g^2 \delta^2 (\Delta - \frac{\delta}{3}) D}$  written as:  $S = S_0 e^{-BD}$

for measuring the diffusion coefficient where  $S$  is the measured NMR signal intensity,  $S_0$  is the measured signal intensity in the absence of diffusion effects (e.g., the signal measured with no field gradients applied) and b)  $^1\text{H}$  DOSY processing, where two diffusive species are observed.

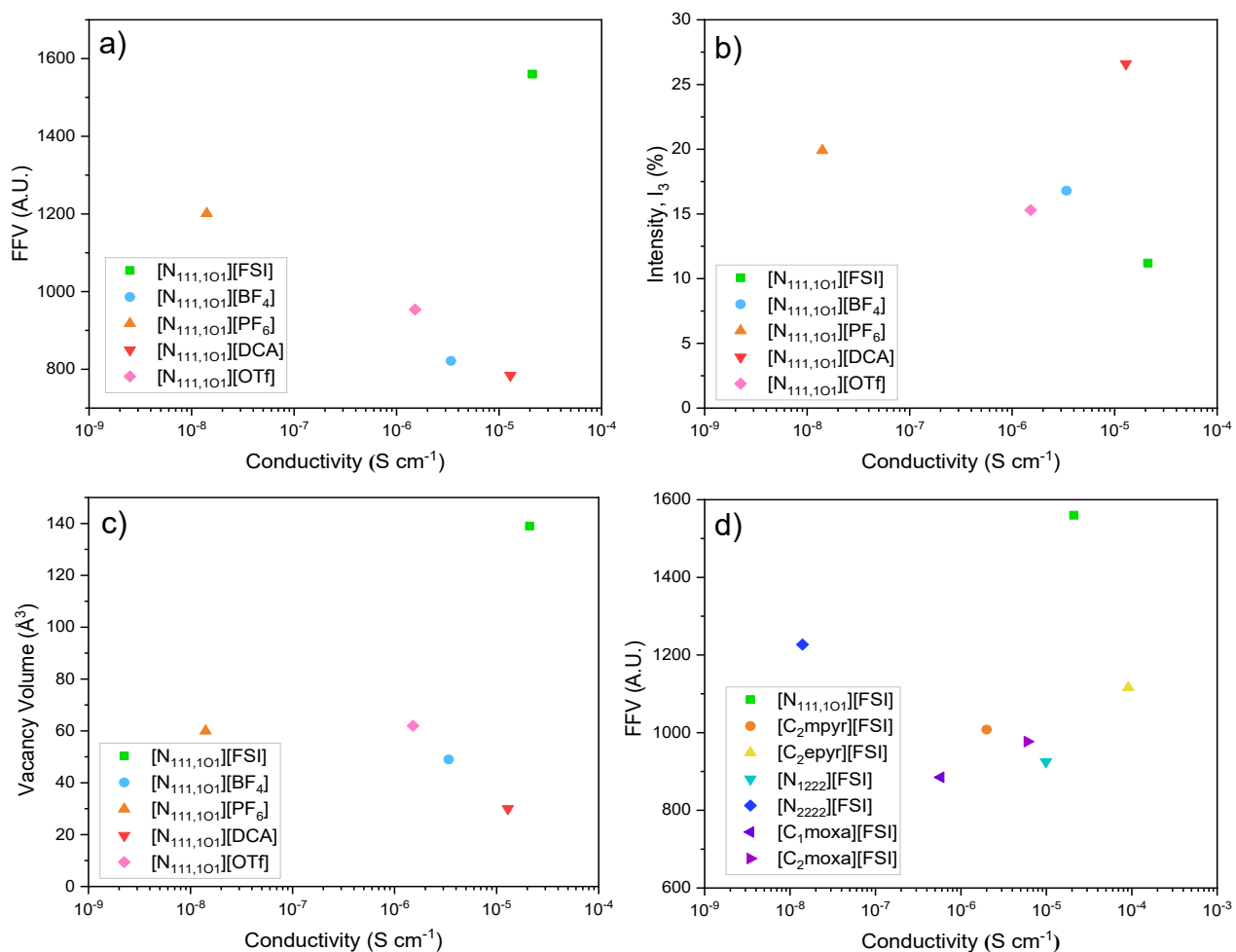


**Figure S12.** The relationship between conductivity of the OIPCs and a) the average fractional free volume (FFV) as determined by PALS, b) Intensity,  $I_3$  (%) (defect concentration), c) vacancy volume ( $\text{\AA}^3$ ) and d) FFV of FSI-based salts in literature.<sup>1-3</sup> PALS analysis in this study were performed at room temperature.

## REFERENCES

- 1 R. Yunis, A. F. Hollenkamp, C. Forsyth, C. M. Doherty, D. Al-Masri and J. M. Pringle, Organic salts utilising the hexamethylguanidinium cation: The influence of the anion on the structural, physical and thermal properties, *Phys. Chem. Chem. Phys.*, 2019, **21**, 12288–12300.
- 2 R. Yunis, D. Al-Masri, A. F. Hollenkamp, C. M. Doherty, H. Zhu and J. M. Pringle, Plastic Crystals Utilising Small Ammonium Cations and Sulfonylimide Anions as Electrolytes for Lithium Batteries, *J. Electrochem. Soc.*, 2020, **167**, 070529.
- 3 C. S. M. Kang, R. Yunis, O. E. Hutt, J. M. Pringle and C. M. Doherty, Ionic liquids and plastic crystals utilising the oxazolidinium cation : the effect of ether functionality in the ring, *Mater. Chem. Front.*